Dynamic Modelling and Simulation of Microelectromechanical Devices With a Circuit Simulation Program

Timo Veijola*, Heikki Kuisma**, and Juha Lahdenperä**

*Helsinki University of Technology, Circuit Theory Laboratory,
P.O.Box 3000, FIN-02015 HUT, Finland, timo@aplac.hut.fi
**VTI Hamlin, P.O.Box 9, FIN-00421 Helsinki, Finland, juha.lahdenpera@vti.fi

ABSTRACT

Simulation blocks of micromechanical sensors and actuators modelling their dynamic electromechanical and fluidic operation are presented. Due to the electrical equivalent circuit realization the sensor system simulations in the frequency and time domains are possible.

A sample library containing parameterized building blocks of inertial sensors is constructed. These component blocks include models for mass-spring systems, capacitance, electrostatic force and gas-film damping in the air gap. The sample library is written in the modelling language of the circuit simulation program APLAC. As an example, an accelerometer model is constructed of the components in the sample library, and its characteristics are simulated in the frequency and time domains.

Keywords: Simulation model, electrical equivalencies, gas-film damping, squeezed-film damping, accelerometer model, block models.

INTRODUCTION

Microlectromechanical sensor and actuator systems are described by complex, dynamic, nonlinear equations in several energy domains. Static responses can be solved in a straightforward manner separately with tools specially designed for, e.g., electrical, mechanical, fluidic, or thermal domains. However, accurate simulation of the dynamics of such complete systems requires concurrent analysis in several energy domains.

As pointed out by Voigt and Wachutka [1], Kirchoffian network theory can be applied in several energy domains. Applying electrical equivalencies, DC, AC and transient responses of such nonlinear, dynamic microelectromechanical sensors and actuators can be solved with a general purpose circuit simulation program. It is then a straightforward task to include the interfacing electronics in the circuit and expand the simulation to complete sensor systems. In addition to the standard analyses, advanced circuit simulators, e.g. APLAC [2], offer noise, sensitivity, stability and oscillator analyses, Monte Carlo, harmonic balance and electro-thermal simulation and optimization.

ELECTRICAL EQUIVALENCIES

The well-known electrical equivalencies for the mechanical and fluidic domains are used here: the voltage / current pair corresponds to velocity / force, pressure / mass flow or temperature / heat flow. Inverse equivalencies can also be described by means of a gyrator component. In practice, additional quantities can be described with equivalent voltages, e.g., mechanical displacement, which acts as a controlling voltage of other component blocks. When the models are nonlinear, scaling the equivalent voltages to levels used in semiconductor components will aid the iteration process.

An electrical equivalent circuit approach has been used successfully in the modelling and simulation of a capacitive accelerometer [3], [4] and an angular rate sensor [5].

PARAMETERIZED COMPONENTS

Parameterized component blocks, or macro components, are frequently used in circuit simulators. The blocks allow any nonlinear, static or dynamic relations to be defined, or existing macro components can be used to build any of these blocks. Similar blocks are useful in creating models for micromechanical devices, too. These models have interfacing nodes that can be connected to other component models, and parameters that are either empirical or they represent physical properties, e.g. dimensions, of the device. The designer can select from several implementation levels making a compromise between accuracy and analysis speed, and can also construct new devices without knowing the details of every component block.

The component parameters usually consist of constant coefficients describing a certain device. Circuit simulators support parameter libraries for such components. The model parameters can also be variable, enabling parameter sweeps, or the values for the variable parameters can be extracted from measurements with optimization algorithms, available in advanced circuit simulators. Their parameters can also be extracted from the simulation results of more complete models. This enables the use of approximate, relatively simple and computationally efficient parameterized models to simulate complete sensor systems.

Table 1: A summary of the components in the sample library. The syntax and parameters show the fixed APLAC syntax and the optional model parameters, respectively. The implementation level controls the accuracy / speed of the model.

Syntax	Parameters	Description/Level	Model equations/blocks

`Reso`
`+ "name"`
`+ nv nv0`
`+ nz nz0`
`+ ...`
	Mass M
	Elastisity κ
	Viscosity γ
		Mechanical mass-spring system
		1: Single mass resonator
		2: Dual mass coupled resonator [5]
			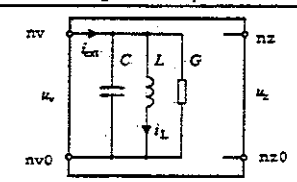

`GapCap`
`+ "name"`
`+ nc nc0`
`+ nz nz0`
`+ ...`
	Mass length l
	Mass width w
	Gap height d
	Beam length b
	Diel. constant ϵ
	Stray cap. C_0
		Capacitance (charge) of the gap
		1: Linear motion
		2: Tilting motion
			$q_G = f(l, w, b, d, \epsilon, C_0, u_z, u_c)$
			 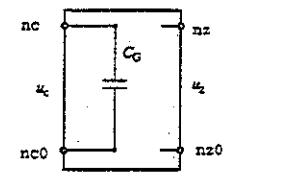

`GapForce`
`+ "name"`
`+ nv nv0`
`+ nz nz0`
`+ nc nc0`
`+ ...`
	Mass length l
	Mass width w
	Gap height d
	Beam length b
	Diel. constant ϵ
		Electrostatic force in the gap
		1: Linear motion
		2: Tilting motion
			$i_{el} = f(l, w, b, d, \epsilon, u_z, u_c)$
			 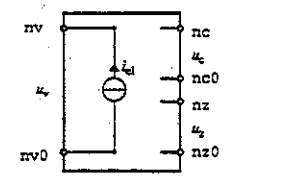

`GasFilm`
`+ "name"`
`+ nv nv0`
`+ nz nz0`
`+ ...`
	Mass length l
	Mass width w
	Gap height d
	Gas viscosity η
	Beam length b
	Mean free path λ
	Accomm. coeff α
	Pressure P_a
	Temperature T
		Gas film model
		1: Rectangular, parallel plates [3], [6], [7]
		2: Rectangular, tilting plates [3], [6], [7]
		3: Finite difference model [4], [6], [7]
			$L_{ij} = f(i, j, l, w, b, d, P_a, T, u_z)$
			$R_{ij} = f(i, j, l, w, b, d, \eta_{eff}, u_z)$
			$\eta_{eff} = f(\eta, \lambda, d, P_a, \alpha, T, u_z)$
			 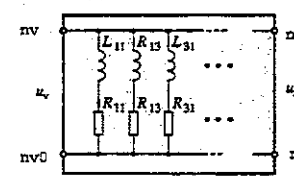

SAMPLE LIBRARY OF COMPONENT BLOCKS

Table 1 summarizes the sample library components consisting of building blocks of capacitive inertial sensors. Electric, mechanical and fluidic energy domains are utilized in these components.

The library components are nonlinear, large-signal models, but currently the gas flow model is accurate only if the pressure and displacement variations are small compared with their static values. The validity of these library components has been tested with measurements of accelerometers and angular rate sensors manufactured by VTI Hamlin.

The sample library is written in the APLAC modelling language and it is external to the simulation program itself.

Resonator

Component `Reso` models one resonance mode of a mass-spring system with an LC resonance circuit shown in Fig. 1. If other than basic resonance modes are of interest, a resonator is needed for each mode. Both linear and rotating modes are modelled with identical resonator circuits.

The linear mode resonator realizes the equation of harmonic motion,

$$M \cdot \frac{\partial^2 z}{\partial t^2} + \gamma \cdot \frac{\partial z}{\partial t} + \kappa \cdot z = F_{ext}, \qquad (1)$$

where γ and κ are the viscosity and elasticity coefficients, respectively, of the cantilever beams. F_{ext} is an external force acting on the mass due to mechanical acceleration $M \cdot a$ and an electrostatic force F_{el}.

When a rotating mode is modelled, the tilting angle θ replaces the displacement z in Eq. (1).

$$I \cdot \frac{\partial^2 \theta}{\partial t^2} + \gamma_I \cdot \frac{\partial \theta}{\partial t} + \kappa_I \cdot \theta = \tau_{ext}, \tag{2}$$

where I, γ_I and κ_I are the moment of inertia, the torsional viscosity and elasticity coefficients, respectively. τ_{ext} is an external twisting moment acting on the mass.

The node voltage u_v equals the velocity v (angular velocity ω) of the mass and voltage $u_z = Li_L$ is proportional to the mass displacement $z = \alpha_s u_z$ (tilting angle θ). An external force F_{ext} (twisting moment τ_{ext}), or acceleration, applied to the mass equals current i_{ext} flowing in the resonator circuit.

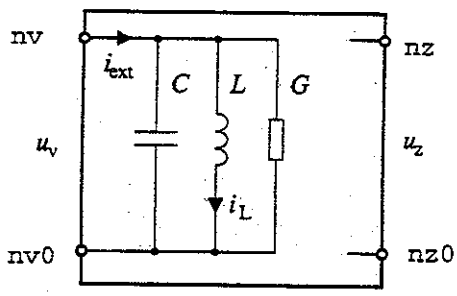

Figure 1: The resonator circuit modelling one resonance mode of a mass-spring system.

Gap Capacitance

Component GapCap models the capacitance in the air gap between two rectangular plates having length l and width w. The capacitance C_G is a function of the displacement z (proportional to voltage u_z). Figure 2 shows the block model of the gap capacitance.

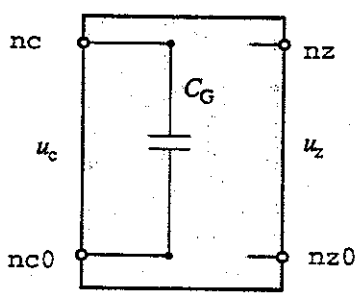

Figure 2: The gap capacitance model. The capacitor charge q_G is controlled by its voltage u_c and the displacement voltage u_z.

The capacitance equation for parallel surfaces moving normal to the surface plane is

$$C_G = \frac{\epsilon w l}{d - z} + C_0, \tag{3}$$

where d is the gap height, ϵ is the dielectric constant and C_0 is the stray capacitance. This model is valid when the mass is supported symmetrically. If the mass is supported from one side only (see Fig. 6) the capacitance is a function of the tilting angle θ [8].

$$C_G = \frac{\epsilon w}{\theta} \ln \left[\frac{d - b\theta}{d - a\theta} \right] + C_0, \tag{4}$$

where b is the length of the supporting bar and $a = b + l$.

Electrostatic Force

Component GapForce models the electrostatic force in the air gap between two rectangular surfaces. Force F_{el} acting on the surfaces is a function of the voltage across the gap u_c and the displacement z. Figure 3 shows the block model of the force source (or twisting moment source).

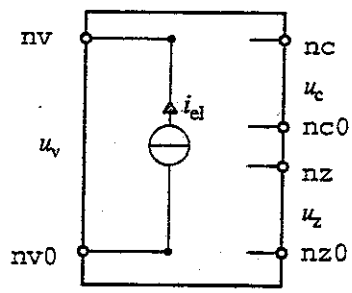

Figure 3: Electrostatic force model.

The force equation for parallel surfaces moving normal to the surfaces is

$$F_{el} = \frac{\epsilon w l u_c^2}{2(d - z)^2}. \tag{5}$$

For tilting surfaces, the twisting moment τ_{el} is function of the tilting angle θ,

$$\tau_{el} = \frac{\epsilon w u_c^2}{2\theta^2} \left\{ \frac{l\theta d}{[d - a\theta]\,[d - b\theta]} - \ln \left[\frac{d - b\theta}{d - a\theta} \right] \right\}. \tag{6}$$

This force also introduces a component $\partial i_{el}/\partial u_z$, that changes, in effect, the spring constant.

Gas-Film Damping

Component block GasFilm models gas flow in the air gap. The model is based on the solution of the linearized Reynolds equation for isothermal conditions. It includes the influence of the rarefied gas flow with a surface quality factor [6], [7] and it is valid in all damping regions from viscous to molecular flow.

When inverse equivalencies for fluid flow quantities are applied, the solution of the Reynolds equation for rectangular plates moving perpendicularly with respect to the surfaces can be realized with the simple equivalent circuit shown in Fig 4. The model consists of an infinite number of RL-sections, but in practice 1–3 sections provide sufficient accuracy.

For small displacements the components R_{ij} and L_{ij} are constant, but when displacement u_z is large, these

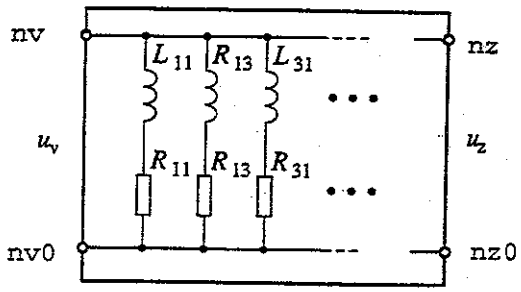

Figure 4: The gas-film damping model for rectangular geometry.

components are controlled by u_z, in which case the mean free path varies and makes the effective viscosity η_{eff} to depend on voltage u_z. The component values are

$$R_{ij} = (ij)^2 \left(\frac{i^2}{w^2} + \frac{j^2}{l^2}\right) \frac{\pi^6 (d-z)^3}{768 l w \eta_{\text{eff}}}, \tag{7}$$

$$L_{ij} = (ij)^2 \frac{\pi^4 (d-z)}{64 l w P_a}, \tag{8}$$

where P_a is the static pressure and i and j are odd integers.

The effective viscosity η_{eff} in Eq. (7) depends on the gap height and the mean free path of λ of the gas through the Knudsen number $K_n = \lambda/d$. An expression for the effective viscosity is given in [6],[7]. The influence of the surface accommodation coefficient α is included in the model. Temperature dependencies are also included in the damping model through the temperature dependencies of the viscosity and mean free path.

For other than rectangular geometries, a more general finite-difference model can alternatively be used, see Fig. 5. Direct equivalencies are applied to realize the finite difference mesh. A gyrator component is required to convert the total pressure into the current that is fed at the velocity node. The synthesis of such an equivalent circuit is discussed in [4].

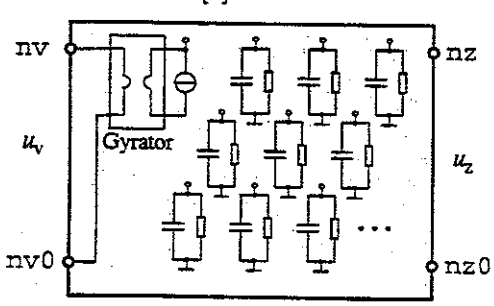

Figure 5: The gas-film damping model realized with a finite difference component mesh.

SAMPLE DEVICE MODELS

Capacitive Accelerometer

In Fig. 6, the structure and cross-section of a silicon micromechanical accelerometer [9] is presented. The

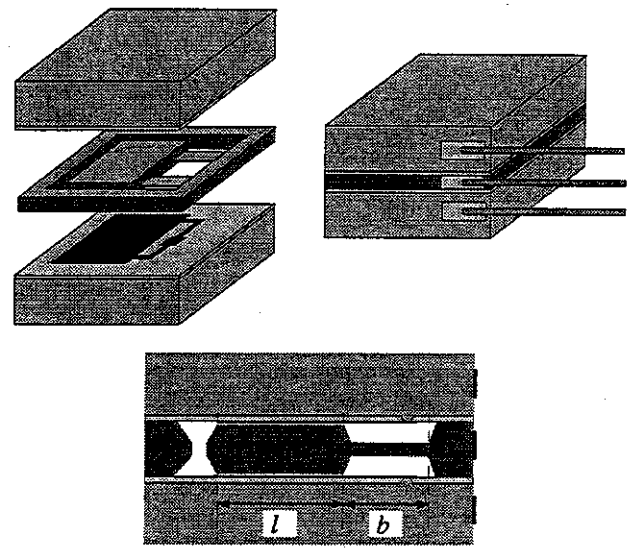

Figure 6: The structure and cross-section of the micromechanical accelerometer produced by VTI Hamlin.

mass and two cantilever beams are anisotropically etched into a silicon wafer.

Figure 7 shows the simulation model built of one resonator and two air gaps [3]. Both air gaps consist of a capacitance, electrostatic force and squeezed-film damping blocks.

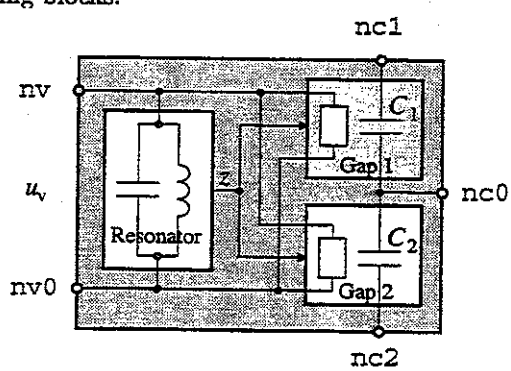

Figure 7: The accelerometer model constructed of one resonator and two air gaps.

The following lines of APLAC code demonstrate how the accelerometer model in Fig. 7 is built using the component blocks in the sample library.

```
DefModel "Accel" 5 nc1 nc2 nc0 nv nv0 PARAM ...
 Reso "LC" nv nv0 nz nz0 MODEL ...
 $ Air gap 1
 GasFilm "SQ1" nv nv0 nz nz0 MODEL ...
 GapCap "C1" nc1 nc0 nz0 nz MODEL ...
 GapForce "F1" nv nv0 nc1 nc0 nz nz0 MODEL ...
 $ Air gap 2
 GasFilm "SQ2" nv nv0 nz0 nz MODEL ...
 GapCap "C2" nc2 nc0 nz nz0 MODEL ...
 GapForce "F2" nv nv0 nc1 nc0 nz0 nz MODEL ...
EndModel
```

Angular Rate Sensor

An angular rate sensor based on a micromechanical dual torsional mass system is modelled with components from the sample library. Three dual-mass resonators model the lowest torsional and linear modes of the system. Additionally, eight air gap models are needed [5].

ACCELEROMETER MODEL SIMULATION EXAMPLES

In the following, the model for the capacitive accelerometer shown in Fig. 7 is simulated with DC, AC and transient analyses. The simulation setups are shown in Fig. 8.

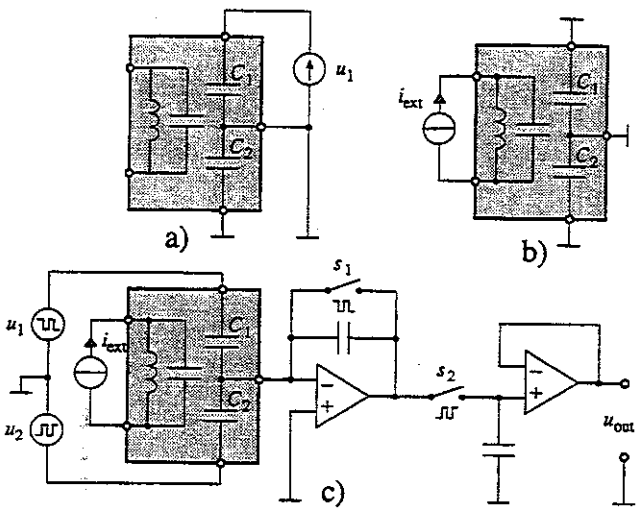

Figure 8: The accelerometer model simulation setups for a) DC, b) AC analyses and for c) transient simulation of an accelerometer system.

DC Analysis

An electrostatic actuation with a variable DC bias voltage source u_1 is connected across the accelerometer's air gap in order to deflect the mass, as shown in Fig. 8a). With this setup, the displacement and capacitance are simulated with respect to the bias voltage (`bias`). The simplified circuit netlist is

```
Accel "A1" n1 0 0 nv 0 ...
Volt  "u1" n1 0 DC=bias R=10k
```

The simulated capacitance-voltage characteristics are shown in Fig. 9.

AC Analysis

In Fig. 8b) an AC current source i_{ext} modelling an external force excitation is connected to the accelerometer model. The simplified APLAC netlist required in analyzing the frequency response of an accelerometer is

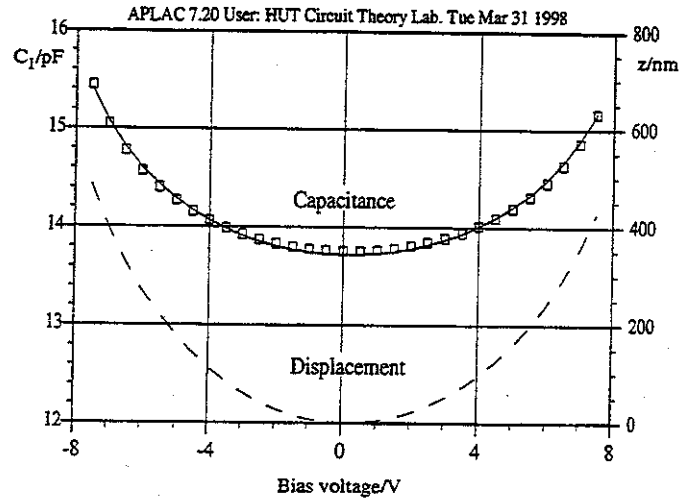

Figure 9: The simulated (——) and measured (□) accelerometer capacitance-voltage characteristics, and the simulated mass displacement (– – –).

```
Accel "A1"  0 0 0 nv 0 MODEL ...
Curr "Iext" 0 nv AC=44u
```

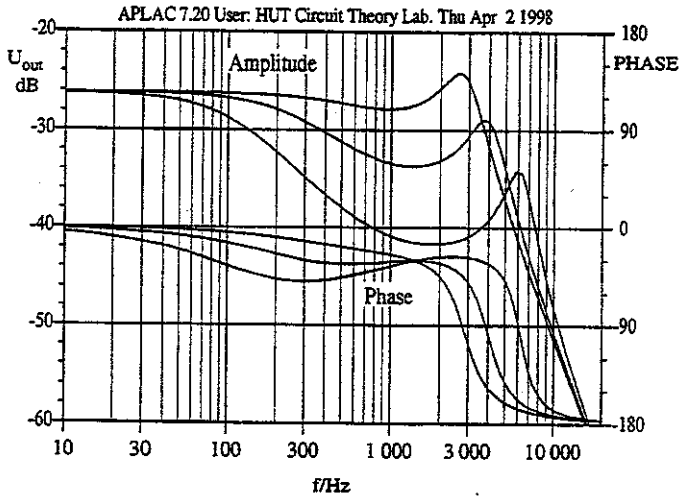

Figure 10: The frequency response of an accelerometer at three pressures.

In this simulation the gap capacitances are not needed. The mass displacement equals the node voltage u_z. Figure 10 shows the simulated and measured accelerometer frequency response at three pressures.

Transient Analysis

Figure 8c) shows the accelerometer model that is connected to a charge amplifier circuit. An acceleration step of 2 g is applied at 50 μs as an external current i_{ext}. The voltage clock sources u_1 and u_2 and the swithes

s_1 and s_2 operate at 50 kHz. The transient simulation of the sensor system at three pressures in Fig. 11 show typical step responses of the gas-damped structure.

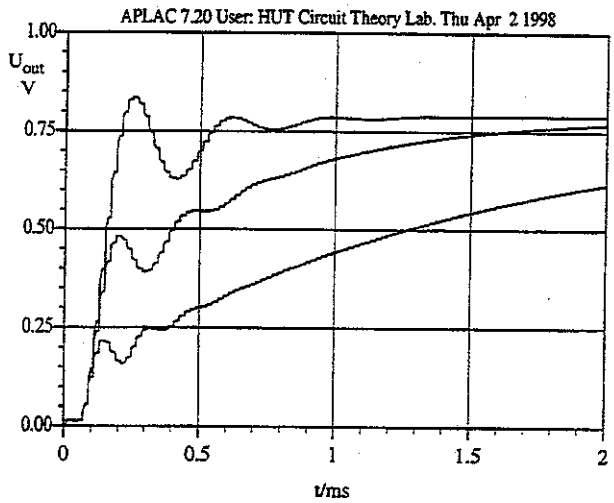

Figure 11: Transient responses at three pressures of the circuit shown in Fig. 8c).

Pressure Distribution

With the aid of the finite difference model, referring to Fig 5, the pressure distribution in the air gap surface can be analyzed. Figure 12 shows the pressure amplitude distribution in the case when the mass has five rectangular holes. The influence of rounded corners is also included. Internal node voltages in the component equal pressure values at the grid points. Mesh size in this example is 30 × 40.

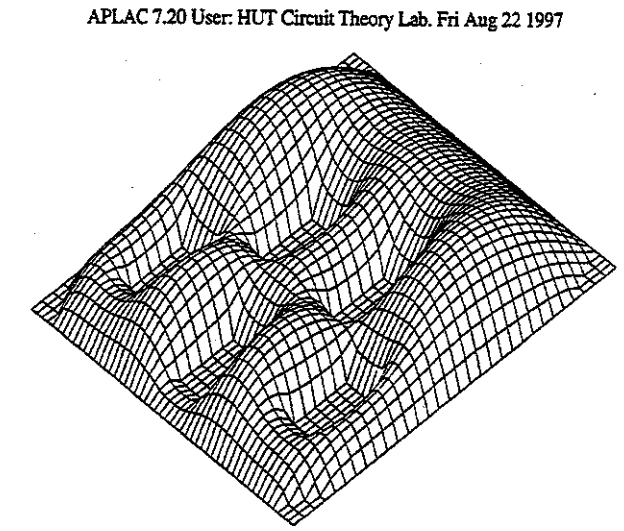

Figure 12: The pressure amplitude distribution on the accelerometer's mass surface solved with an electrical equivalent finite difference model.

CONCLUSIONS

Dynamic, nonlinear electrical equivalent circuit models for microelectromechanical structures and their simulation with a circuit simulation program were discussed. It was emphasized that several standard properties of advanced circuit simulation programs are useful in dynamic simulation of sensors and actuators, too. A sample component library of building blocks for silicon capacitive inertial sensors was presented. With this sample library, more complex inertial sensor systems, including, e.g., force feedback, can be built and simulated in a straightforward manner. Using similar macro modelling approach, the library can be extended to model any kind of microelectromechanical devices and systems.

REFERENCES

[1] P. Voigt and G. Wachutka, "Electro-fluidic microsystem modeling based on Kirchoffian network theory," in *Proceedings of Transducers'97*, (Chicago), pp. 1019–1022, June 1997.

[2] M. Valtonen *et al.*, *APLAC*. Helsinki University of Technology and Nokia Research Center, 7.1 Reference Manual and 7.1 User's Manual, Otaniemi, Oct. 1997. http://www.aplac.hut.fi/aplac.

[3] T. Veijola, H. Kuisma, J. Lahdenperä, and T. Ryhänen, "Equivalent circuit model of the squeezed gas film in a silicon accelerometer," *Sensors and Actuators A*, vol. 48, pp. 239–248, 1995.

[4] T. Veijola, T. Ryhänen, H. Kuisma, and J. Lahdenperä, "Circuit simulation model of gas damping in microstructures with nontrivial geometries," in *Proceedings of Transducers'95 and Eurosensors IX*, vol. 2, (Stockholm), pp. 36–39, June 1995.

[5] T. Veijola, H. Kuisma, J. Lahdenperä, and T. Ryhänen, "Simulation model for micromechanical angular rate sensor," *Sensors and Actuators A*, vol. 60, pp. 113–121, 1997.

[6] T. Veijola, H. Kuisma, and J. Lahdenperä, "Model for gas film damping in a silicon accelerometer," in *Proceedings of Transducers'97*, (Chicago), pp. 1097–1100, June 1997.

[7] T. Veijola, H. Kuisma, and J. Lahdenperä, "The influence of gas-surface interaction on gas film damping in a silicon accelerometer," *Sensors and Actuators A*, vol. 66, pp. 83–92, 1998.

[8] T. Veijola and T. Ryhänen, "Model of capacitive micromechanical accelerometer including effect of squeezed gas film," in *Proceedings of the 1995 IEEE International Symposium on Circuits and Systems*, (Seattle), pp. 664–667, 1995.

[9] J. Lahdenperä and U. Meriheinä, "A low cost high performance capacitive accelerometer," in *Proceedings of Sensor '91*, vol. 3, (Nürnberg), p. 235, 1991.